



Published in final edited form as:

Int J Radiat Oncol Biol Phys. 2013 May 1; 86(1): 136–142. doi:10.1016/j.ijrobp.2012.12.007.

Imaging primary mouse sarcomas after radiation therapy using cathepsin-activatable fluorescent imaging agents

Kyle C. Cuneo, MD¹, Jeffrey K. Mito, BA², Melodi P. Javid, BS², Jorge M. Ferrer, PhD³, Yongbaek Kim, DVM, PhD⁴, W. David Lee, MS⁵, Mounji G. Bawendi, PhD³, Brian E. Brigman, MD, PhD⁶, and David G. Kirsch, MD, PhD^{1,2,*}

¹Department of Radiation Oncology, Duke University School of Medicine, Durham, NC 27710

²Department of Pharmacology and Cancer Biology, Duke University School of Medicine, Durham, NC 27710

³Department of Chemistry, Massachusetts Institute of Technology, Cambridge, MA 02140

⁴Department of Clinical Pathology, College of Veterinary Medicine, Seoul National University, Seoul 156-707, Republic of Korea

⁵The David H. Koch Institute for Integrative Cancer Research, Massachusetts Institute of Technology, Cambridge, MA 02140

⁶Department of Orthopedic Surgery, Duke University School of Medicine, Durham, NC 27710

Abstract

Purpose—Cathepsin-activated fluorescent probes can detect tumors in mice and in canine patients. We previously showed that these probes can detect microscopic residual sarcoma in the tumor bed of mice during gross total resection. Many patients with soft tissue sarcoma (STS), and other tumors, undergo radiation therapy (RT) prior to surgery. This study assesses the effect of RT on the ability of cathepsin-activated probes to differentiate between normal and cancerous tissue.

Methods and Materials—A genetically engineered mouse model of STS was used to generate primary hind limb sarcomas that were treated with hypofractionated RT. Mice were injected intravenously with cathepsin-activated fluorescent probes and various tissues, including the tumor, were imaged using a handheld imaging device. Resected tumor and normal muscle samples were harvested to assess cathepsin expression by western blot. Uptake of activated probe was analyzed by flow cytometry and confocal microscopy. Parallel *in vitro* studies using mouse sarcoma cells were performed.

Results—RT of primary STS in mice and mouse sarcoma cell lines caused no change in probe activation or cathepsin protease expression. Increasing radiation dose resulted in an upward trend in probe activation. Flow cytometry and immunofluorescence showed that a substantial proportion of probe-labeled cells were CD11b positive tumor associated immune cells.

Conclusions—In this primary mouse model of STS, RT does not affect the ability of cathepsin-activated probes to differentiate between tumor and normal muscle. Cathepsin-activated probes label tumor cells and tumor associated macrophages. Our results support including patients who have received preoperative RT in clinical studies evaluating cathepsin-activated imaging probes.

*David G. Kirsch, M.D., Departments of Radiation Oncology and Pharmacology and Cancer Biology, Duke University School of Medicine, Duke University Medical Center, Durham, NC 27710. Tel: 919-681-8586; Fax: 919-681-1867; david.kirsch@duke.edu.

Conflicts of Interest Notification: DGK is a consultant as a member of the scientific advisory board for Lumicell Diagnostics, a company commercializing intraoperative imaging systems. MGB and WDL are founders of Lumicell Diagnostics. WDL and JMF are currently employees of Lumicell Diagnostics. MGB, JMF, WDL, and DGK have submitted a patent for the handheld imaging device.

Introduction

Soft tissue sarcoma (STS) of the extremity is commonly treated with limb sparing surgery. In patients undergoing limb sparing procedures, the use of adjuvant radiation therapy (RT) improves local control from approximately two-thirds to 90% (1-3). Prior reports have suggested that, compared to postoperative RT, preoperative RT is associated with increased rates of wound complications, but less subcutaneous fibrosis, joint stiffness, and edema with no significant change in local control or survival (4-5). Therefore, preoperative RT is often used to treat patients with a high grade STS of the extremity.

When a sarcoma is resected, a pathologist examines the resected tumor and determines if cancer is present at the inked surgical margin. If tumor cells extend to the edge of the specimen, the margin is considered positive. A positive margin is associated with increased rates of local recurrence and reoperation (6). This method is prone to sampling error as only a small fraction of the resected tumor is inspected. Furthermore, because the tumor bed is not examined, this method may miss skip lesions or tumor cells that have contaminated the tumor bed during surgery.

A wide field-of-view imaging system has been developed to detect microscopic residual cancer in a surgical tumor bed using a handheld device that detects near infrared (NIR) fluorescence (7). The imaging device has a spatial resolution of approximately 16 microns and a field of view of 9.0 mm by 6.6 mm, allowing one to scan a tumor bed quickly. The system has been optimized to detect NIR light, allowing for relatively increased tissue penetration. Prosense 680 and VM249 are cathepsin-activated fluorescent probes that emit a NIR signal when their peptide backbone is cleaved by cysteine proteases including cathepsins B and L. By using the handheld imaging device, small clusters of cells which have activated VM249 or Prosense 680 can be detected in a tumor bed after surgical resection (7).

Because cathepsin proteases are preferentially expressed in STS compared to adjacent skeletal muscle (7), a cathepsin-activated fluorescent probe can provide signal contrast between the normal tissue and tumor. Preclinical studies have shown that this imaging system can detect cancer in a primary mouse model of STS (7) and spontaneous cancers in canine patients (8). In the mouse sarcoma model (9), the presence of NIR signal in the tumor bed correlates with microscopic residual sarcoma and local recurrence. Furthermore, the removal of tissue with residual fluorescence improves local control (7). Therefore, if this imaging technology can be successfully translated in human clinical trials it has the potential to risk-stratify patients for local recurrence and improve outcomes.

A phase I clinical trial is now underway to test the safety of a cathepsin-activated fluorescent probe in patients with STS (NCT01626066). To determine whether patients receiving preoperative RT should be included in the clinical trial, we performed pre-clinical studies to understand the effect of radiation on the expression of cathepsin proteases, the activation of cathepsin-activated probes, and imaging of primary STS in mice.

Methods

Mouse Model and Irradiation Technique

All animal studies were performed in accordance with IACUC-approved protocols. We used genetically engineered *Braf^{CA}*; *p53^{F1/F1}* or *LSL-Kras^{G12D}*; *p53^{F1/F1}* mice to generate primary STS as previously described (9). Once tumors were approximately 5-10 mm in greatest dimension, the mice were treated with RT to the involved hind limb. Radiation was administered in 5 Gy daily fractions to a total dose of 0, 5, 15, or 25 Gy using a single field

from a XRAD 320 Biological Irradiator (Precision X-ray, North Branford, CT) at a dose rate of 2-2.2 Gy/min with 320 kVp photons at 12.5 mA using a 2.5 mm Al/0.1 mm Cu filter. Three orthogonal tumor dimensions were measured at regular intervals and volumes were calculated using the following equation: $\text{Volume} = \pi/6 (\text{Dimension 1} * \text{Dimension 2} * \text{Dimension 3})$. Tumor volume was compared among groups using the Student's t-test.

Imaging

One week after finishing RT, mice were administered 2 nmol of VM249 (PerkinElmer, San Jose, Ca) in 100 μL of PBS via tail vein injection. Six hours after injection, the mice were killed and the STS were resected. The surgical margin was inked and muscle from the contralateral hind limb was harvested. The tumor, contralateral muscle, and tumor bed were imaged using the handheld imaging device (Lumicell Diagnostics, Waltham, MA). Images were analyzed as previously described (7). The mean signal intensity was also calculated to determine the tumor to muscle signal ratio and the tumor to tumor bed signal ratio for each group (n = 4-5). Additionally, the inked tumor margin from the resected specimen was subjected to conventional histopathological analysis.

Western Blot Analysis

Protein isolated from tissue or cell lines was resolved on a SDS-PAGE gel (Biorad Laboratories, Hercules, CA) and membranes were probed with anti-Cathepsin B (sc-6493) and L (sc-6501) antibodies (Santa Cruz Biotechnology, Santa Cruz, CA). Anti-GAPDH antibody (G9545, Sigma-Aldrich, St. Louis, MO) was used as a loading control.

Imaging individual cells placed over a simulated tumor bed

Mice bearing primary STS were injected with 2 nmol Prosense 680 (PerkinElmer, San Jose, Ca) via tail vein injection. The sarcoma was resected twenty-four hours later and the tumor was homogenized with trypsin, collagenase IV, dispase (Invitrogen) and passed through a strainer to separate the tumor aggregate into individual cells. Single cells were sorted for Prosense (+) signal using flow cytometry (FACSVantage; Becton Dickinson, Franklin Lakes, NJ) and single cell suspensions were stored in PBS on ice. Within 2 hours, a simulated tumor bed was generated in recipient mice with or without prior Prosense 680 injection by exposing the gluteal muscle with a scalpel. Fifty μL of the cell suspension was deposited over the exposed muscle tissue, while the area was imaged with the device. The brightness and contrast of the fluorescence images were adjusted using recipient mice injected with Prosense 680 and the same settings were applied to images from mice without Prosense 680 injection. For confocal imaging (Leica SP5 Confocal Microscope; Wetzlar, Germany), normal muscle tissue was removed from tumor-free mice 24 hours after Prosense 680 injection and placed over a microscope slide and 50 μL of the cell suspension was placed on top. Confocal images were taken at 20X and 63X magnification.

Immunofluorescent Microscopy

Five to 20 micron thick frozen sections were blocked with serum and incubated with an anti-F4/80 antibody (14-4801, eBioscience, San Diego, CA) followed by an Alexa Fluor 488 labeled secondary antibody (A-21208, Invitrogen, Grand Island, NY). Nuclei were stained with DAPI and slides were imaged by confocal microscopy.

Total Body Irradiation and VM249 Activation in Normal Tissues

Non-tumor bearing *LSL-Kras^{G12D};p53^{Fl/Fl}* mice were treated with total body irradiation at a dose of 720 cGy in 4 daily 180 cGy fractions using the 320 kVp x-ray source described above. One week later, irradiated and unirradiated mice were intravenously injected with 2 nmol VM249 and killed six hours later. Muscle, liver, small bowel, stomach, lung, kidney,

and spleen were removed, washed in PBS, and imaged using the device. The mean signal intensity for each sample was obtained as described previously (7).

In vitro studies

Cells from a primary mouse STS were harvested from a *Braf^{CA};p53^{F1/F1}* mouse, purified, and cultured in DMEM with 10% fetal bovine serum. Sarcoma cells were plated in equal density, grown to 70-80% confluency and irradiated with 0, 2, 4, or 6 Gy using the 320 kVp x-ray source at a dose rate of 2.2 Gy/minute. 24 hours later VM249 was added at a concentration of 0 nM, 500 nM, or 1500 nM. 24 hours later cells were harvested, washed in PBS, and resuspended with propidium iodide in PBS. Cells were analyzed and counted by flow cytometry. Scatter plots were gated and analyzed using FlowJo Software (Ashland, OR).

Results

RT does not compromise NIR signal in a mouse model of STS

Braf^{CA};p53^{F1/F1} mice were used to generate primary hind limb STS expressing *Braf^{V600E}* with *p53* deletion (7). These mice were treated with 0, 5, 15, or 25 Gy in 5 Gy daily fractions and tumor volume was measured every 2-3 days (Figure 1A). At 7 days after completion of RT, mice treated with 15 or 25 Gy showed significant tumor growth delay compared to untreated mice or mice treated with a single 5 Gy fraction (Figure 1B). At this time point, mice were injected with the cathepsin-activated fluorescent probe VM249 and killed 6 hours later when the resected tumor, tumor bed, and contralateral hind limb muscle were imaged using the handheld device (Figure 2A, B). The use of RT did not significantly affect the tumor: muscle signal ratio ($p < 0.173$, control compared to 25 Gy), but there was a trend towards higher tumor: muscle ratio with increasing radiation dose (Figure 2C). The tumor: tumor bed signal ratio was not significantly different for untreated mice or mice treated with 15 or 25 Gy with a histopathologically confirmed negative surgical margin (Figure 2D).

Cathepsin protease expression and in vitro probe activation after RT

Western blot analysis of fresh tissue from mice with and without RT showed that Cathepsin B and L were strongly expressed in the tumor but not the muscle and levels of expression did not change with RT (Figure 3A).

To study the effect of RT on cathepsin expression *in vitro*, mouse STS cells were irradiated with 0, 2, 4, or 6 Gy in a single fraction. Cells were harvested 24 hours later and analyzed by Western blot (Figure 3B). Cathepsin B and L were strongly expressed in tumor cell lines and expression levels did not vary with increasing radiation dose.

In vitro probe activation was assessed by incubating radiation treated cells with VM249. Cells were harvested and flow cytometry was used to quantify the percentage of viable cells labeled with VM249. RT resulted in a small, approximately 2% per Gy, increase in labeling of cells by VM249 (Figure 3C).

Cathepsin-activated probes label tumor parenchymal and immune cells

We examined the *in vivo* localization of activated probe in the tumor bed and in individual cells. Cells were harvested from a sarcoma in a mouse after injection of the cathepsin-activated probe, Prosense 680 (Figure 4A). Prosense(+) cells were isolated and reintroduced into a simulated mouse tumor bed where they were imaged with the handheld device (Figure 4B-E). Prosense(+) cells were also imaged using confocal microscopy revealing a punctate

cytoplasmic distribution, localizing Prosense 680 within organelles, such as lysosomes (Figure 4F).

We then studied probe activation within the native tumor environment by preparing frozen sections of primary STS from irradiated and non-irradiated mice after injection of the cathepsin-activated probe VM249. Fluorescence microscopy of these samples demonstrates both VM249-positive tumor cells and VM249-positive F4/80 stained macrophages (Figure 5A, B).

In a separate experiment, STS were generated in *Rosa26^{YFP/YFP}; LSL-Kras^{G12D}; p53^{F1/F1}* mice. These sarcoma cells express the yellow fluorescent protein (YFP). Mice with STS were injected with the cathepsin-activated probe Prosense 680. Cells were isolated from the tumor and analyzed by flow cytometry. About two-thirds of the Prosense(+) cells were YFP(+) tumor parenchymal cells. About one third of Prosense(+) cells were also positive for CD11b, a marker of tumor associated macrophages (Figure 5D). Together, these results suggest that both sarcoma cells and TAMs are labeled by the cathepsin-activated probes.

Effects of RT on VM249 Activation in Organs

Non-tumor bearing mice were treated with total body irradiation and injected with the cathepsin-activated fluorescent probe VM249. The heart, kidney, liver, lung, spleen, and skeletal muscle were imaged after injection using the handheld imaging device. RT did not significantly alter the amount of signal from VM249 in each organ imaged (Figure 6). High levels of signal were seen in the kidney, which excretes the probe. Skeletal muscle and cardiac muscle demonstrated similar signal intensities.

Discussion

Given the high expression of cathepsin proteases in sarcomas compared to skeletal muscle, cathepsin-activated fluorescent probes are promising agents for intraoperative imaging of STS. We have shown that these probes can be used during surgery in sarcoma-bearing mice to detect residual fluorescence in the tumor bed that correlates with residual cancer cells and local recurrence (7). Based on these results and a clinical trial testing this technology in canine patients with spontaneous tumors (8), a Phase I clinical trial is now open to test the safety of a cathepsin-activated fluorescent probe in humans with STS or breast cancer (NCT01626066).

The utility of cathepsin-activated probes to discriminate between tumor and normal tissue has also been shown in other types of cancer. Eser *et al.* used a mouse model of pancreatic ductal adenocarcinoma to show that a cathepsin-activated NIR probe could detect low-grade lesions and differentiate tumor from normal tissue (10). Furthermore, topically applied cathepsin-based probes have been used *ex vivo* to label human high grade glioma specimens, but not adjacent normal tissue (11).

There are few reports on the effect of RT on cathepsin protease expression and activity in tumors or skeletal muscle. Seo *et al.* studied the effects of radiation on cathepsin S expression in a breast cancer model. In this study, RT transiently induced cathepsin S expression (12). In the current study, cathepsins B and L were expressed at much higher levels in resected mouse sarcoma compared to skeletal muscle or tumor bed *in vivo*. Levels of cathepsins B and L remained constant with increasing radiation dose *in vivo* and *in vitro*. Accordingly, probe activation does not change significantly with RT indicating that activity of cathepsins B and L is not modulated by radiation.

Tumor associated macrophages play an important role in the activation of cathepsin-activated probes in this system as approximately 30% of the cells that activated cathepsin-based probes were CD11b(+). Immunofluorescence studies showed RT independent co-localization of probe to both tumor parenchymal and immune cells. These data suggest that RT does not reduce probe activation by cathepsin proteases expressed by tumor parenchyma or immune cells.

There are several limitations to our preoperative radiation mouse model. The NCCN recommends treatment in 2 Gy fractions to 50 Gy for patients with STS receiving neoadjuvant RT (13). In the current study, mice were treated with 5 Gy fractions from 0 to 25 Gy which is the equivalent 2 Gy dose (EQD₂) of 54 Gy or 40 Gy, assuming an α/β ratio of 10 or 3, respectively. Additionally, there is typically a month break after finishing RT prior to surgery. In this study, tumors in mice were resected after a week because of rapid tumor growth. Finally, this mouse sarcoma model is most similar to undifferentiated pleomorphic sarcoma compared to other STS subtypes (14) and the treatment effect on the mouse sarcomas as assessed by histology appeared to be modest with this dose and schedule of RT. It is possible that for some subtypes of STS, such as myxoid liposarcoma, which are particularly responsive to radiation (15), the effect on cathepsin-activated probes would be more substantial.

Despite these limitations, the imaging system was effective at differentiating tumor from muscle following RT. Following RT, there was a trend towards improved tumor to muscle signal ratio and a nearly identical tumor to tumor bed signal ratio compared to mice without RT. Furthermore, total body irradiation did not significantly alter the signal from VM249 in several types of normal tissue. *In vitro*, radiation resulted in a small increase in VM249 activation in tumor cells. Taken together, these findings indicate that the use of pre-operative RT does not impair the ability of cathepsin-activated imaging probes to preferentially label sarcomas compared to normal muscle. Therefore, this study supports the inclusion of patients treated with preoperative RT in the phase I clinical trial testing this technology.

Acknowledgments

We thank Linda Griffith for helpful discussions, Tyler Jacks for providing the LSL-Kras^{G12D} mice, Martin McMahon for providing the Brat^{Ca} mice, and Anton Berns for providing the p53^{Fl} mice. This work was supported by a Damon Runyon-Rachleff Innovation Award (DGK).

References

1. Yang JC, Chang AE, Baker AR, et al. Randomized prospective study of the benefit of adjuvant radiation therapy in the treatment of soft tissue sarcomas of the extremity. *J Clin Oncol*. 1998; 16:197–203. [PubMed: 9440743]
2. Pisters PW, Harrison LB, Leung DH, et al. Long-term results of a prospective randomized trial of adjuvant brachytherapy in soft tissue sarcoma. *J Clin Oncol*. 1996; 14:859–68. [PubMed: 8622034]
3. Pisters PW, Leung DH, Woodruff J, et al. Analysis of prognostic factors in 1,041 patients with localized soft tissue sarcomas of the extremities. *J Clin Oncol*. 1996; 14:1679–89. [PubMed: 8622088]
4. O'Sullivan B, Davis AM, Turcotte R, et al. Preoperative versus postoperative radiotherapy in soft-tissue sarcoma of the limbs: a randomised trial. *Lancet*. 2002; 359:2235–41. [PubMed: 12103287]
5. Davis AM, O'Sullivan B, Turcotte R, et al. Late radiation morbidity following randomization to preoperative versus postoperative radiotherapy in extremity soft tissue sarcoma. *Radiother Oncol*. 2005; 75:48–53. [PubMed: 15948265]
6. Lewis JJ, Leung D, Casper ES, et al. Multifactorial analysis of long-term follow-up (more than 5 years) of primary extremity sarcoma. *Arch Surg*. 1999; 134:190–4. [PubMed: 10025462]

7. Mito JK, Ferrer JM, Brigman BE, et al. Intraoperative detection and removal of microscopic residual sarcoma using wide-field imaging. *Cancer*. 2012
8. Eward WC, Eward C, Mito JK, et al. Real time in vivo tumor bed assessment following resection of naturally occurring sarcoma in dogs: a canine clinical trial. *CORR*. 2012 In Press.
9. Kirsch DG, Dinulescu DM, Miller JB, et al. A spatially and temporally restricted mouse model of soft tissue sarcoma. *Nat Med*. 2007; 13:992–7. [PubMed: 17676052]
10. Eser S, Messer M, Eser P, et al. In vivo diagnosis of murine pancreatic intraepithelial neoplasia and early-stage pancreatic cancer by molecular imaging. *PNAS*. 2011; 08(24):9945–50. [PubMed: 21628592]
11. Cutter JL, Cohen NT, Wan J, et al. Topical application of activity-based probes for visualization of brain tumor tissue. *PLoS one*. 2012; 7(3):e33060. [PubMed: 22427947]
12. Seo HR, Bae S, Lee YS. Radiation-induced cathepsin S is involved in radioresistance. *International Journal of Cancer*. 2009; 124:1794–1801.
13. NCCN Guidelines: Soft Tissue Sarcoma. 2012
14. Mito JK, Riedel RF, Dodd L, et al. Cross species genomic analysis identifies a mouse model as undifferentiated pleomorphic sarcoma/malignant fibrous histiocytoma. *PLoS One*. 2009; 4:e8075. [PubMed: 19956606]
15. Chung PW, Dehesi BM, Ferguson PC, et al. Radiosensitivity translates into excellent local control in extremity myxoid liposarcoma: a comparison with other soft tissue sarcomas. *Cancer*. 2009; 115(14):3254–61. [PubMed: 19472403]

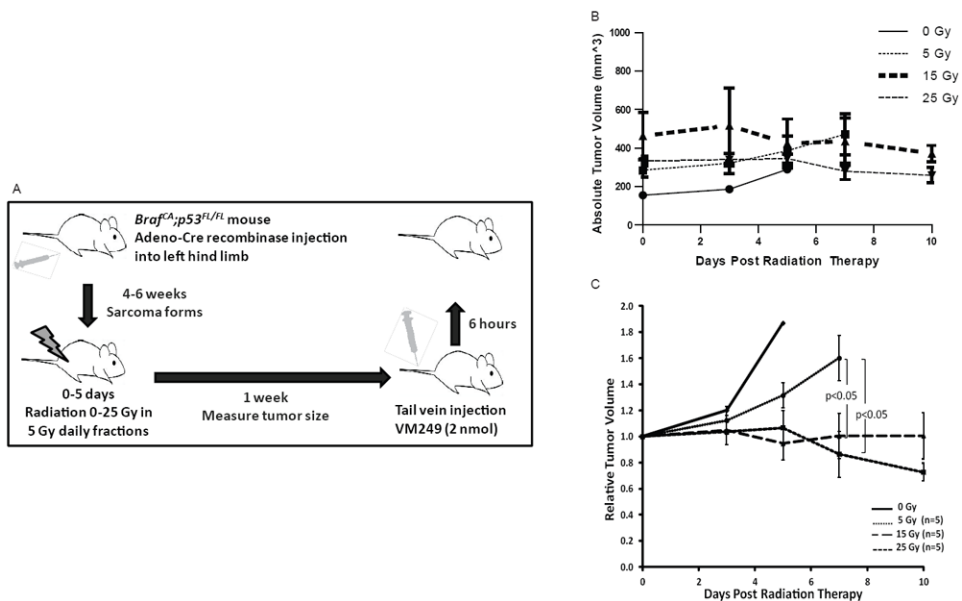


Figure 1. RT causes growth delay in primary STS of the hindlimb in *Braf^{CA}; p53^{FL/FL}* mice. (A) Schematic of method using genetically engineered mice for generation of primary hind limb sarcomas, treatment with RT, and subsequent imaging of the tumor and related tissue. (B) The 3 curves show the fold change in tumor volume after RT.

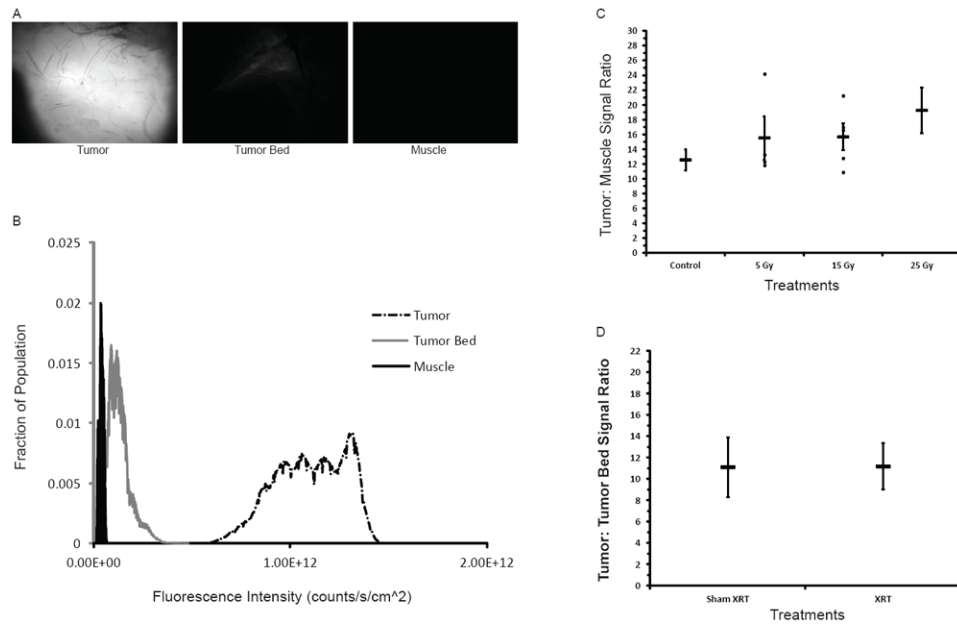


Figure 2. RT does not affect relative imaging signal intensity. VM249 was administered to mice from Fig. 1 and the NIR fluorescent signal from the imaged tissue is represented qualitatively (A) and quantitatively (B) (Exposure = 5 ms). (C) The tumor: normal muscle signal ratio was determined for mice with and without RT. (D) The tumor: tumor bed signal ratio was determined for those tumors with a histologically negative surgical margin.

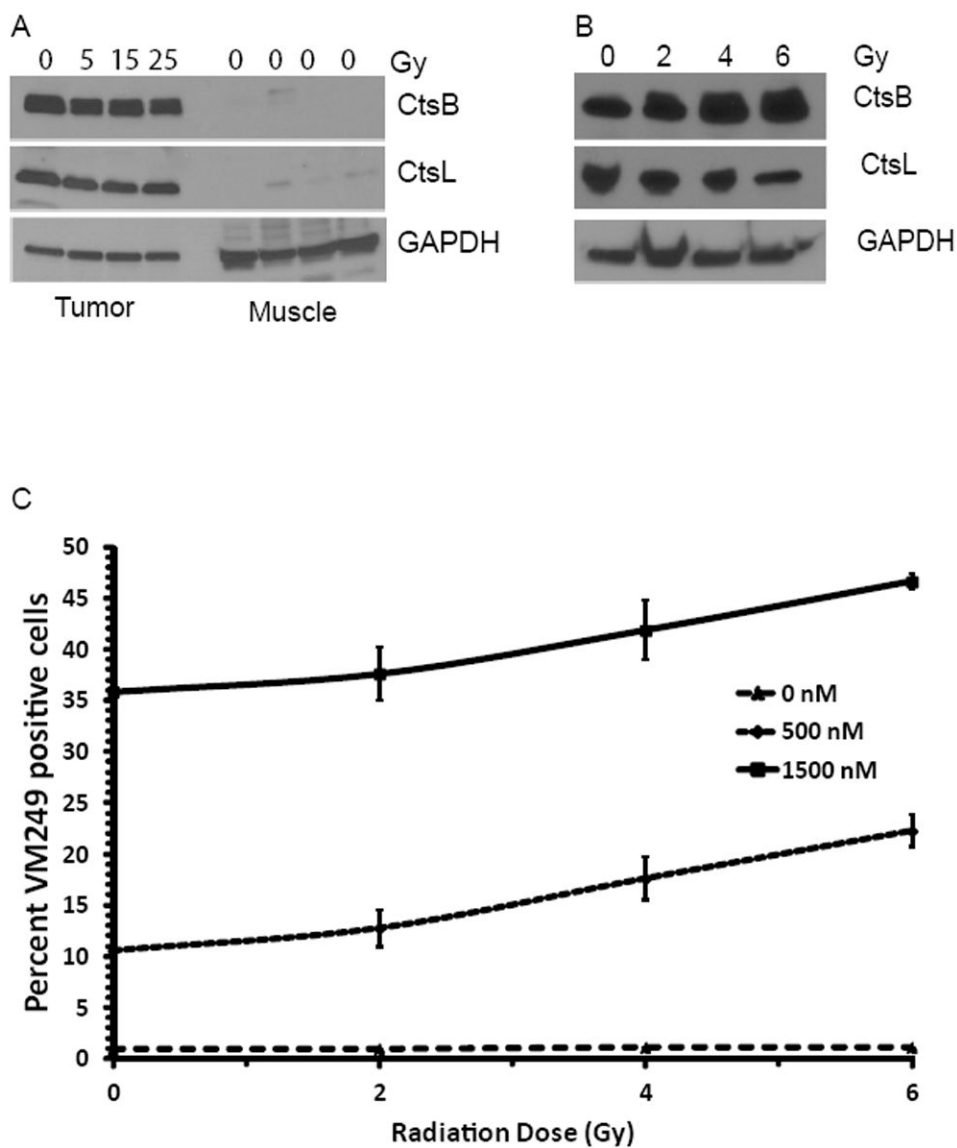


Figure 3. Irradiation does not alter cathepsin expression or probe activation. (A) Cathepsin protein levels found in sarcoma and normal muscle harvested from mice that received 0, 5, 15 or 25 Gy. (B) Cathepsin protein levels representative of several sarcoma cell lines treated with 0, 2, 4 or 6 Gy. (C) Flow cytometric analysis showing the effect of RT on labeling of sarcoma cells by 500 nM or 1500 nM VM249.

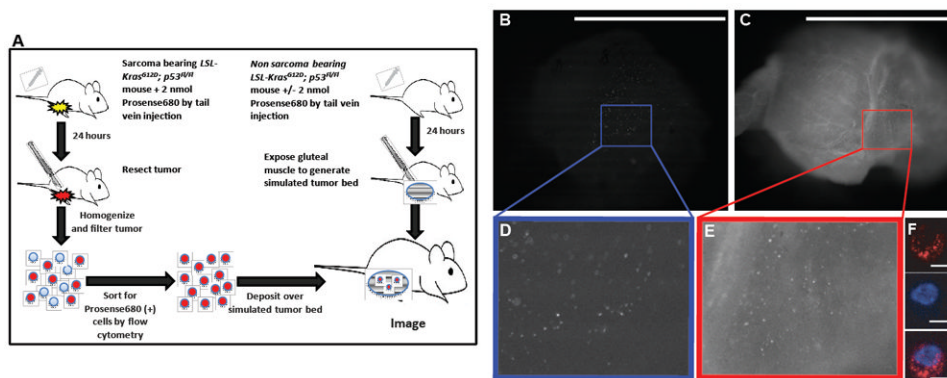


Figure 4.

Imaging individual cells transferred into simulated tumor beds in vivo. (A) Cells were obtained by flow cytometry from a sarcoma bearing mouse 24 hours after Prosense 680 injection. Individual Prosense (+) cells from the sarcoma were detected by the hand-held imaging device when placed in a simulated tumor bed from a mouse not injected (B) and injected (C) with Prosense 680. (F) Prosense signal was confirmed to originate from individual cells by confocal microscopy in the Prosense channel (top, red) and nuclear Hoechst stain (middle, blue), which were merged together (bottom). Insets in A and B show a 2.5x magnification of the highlighted area (D, E). Scale bars: 5 mm for A, B; 10 μ m for D, E.

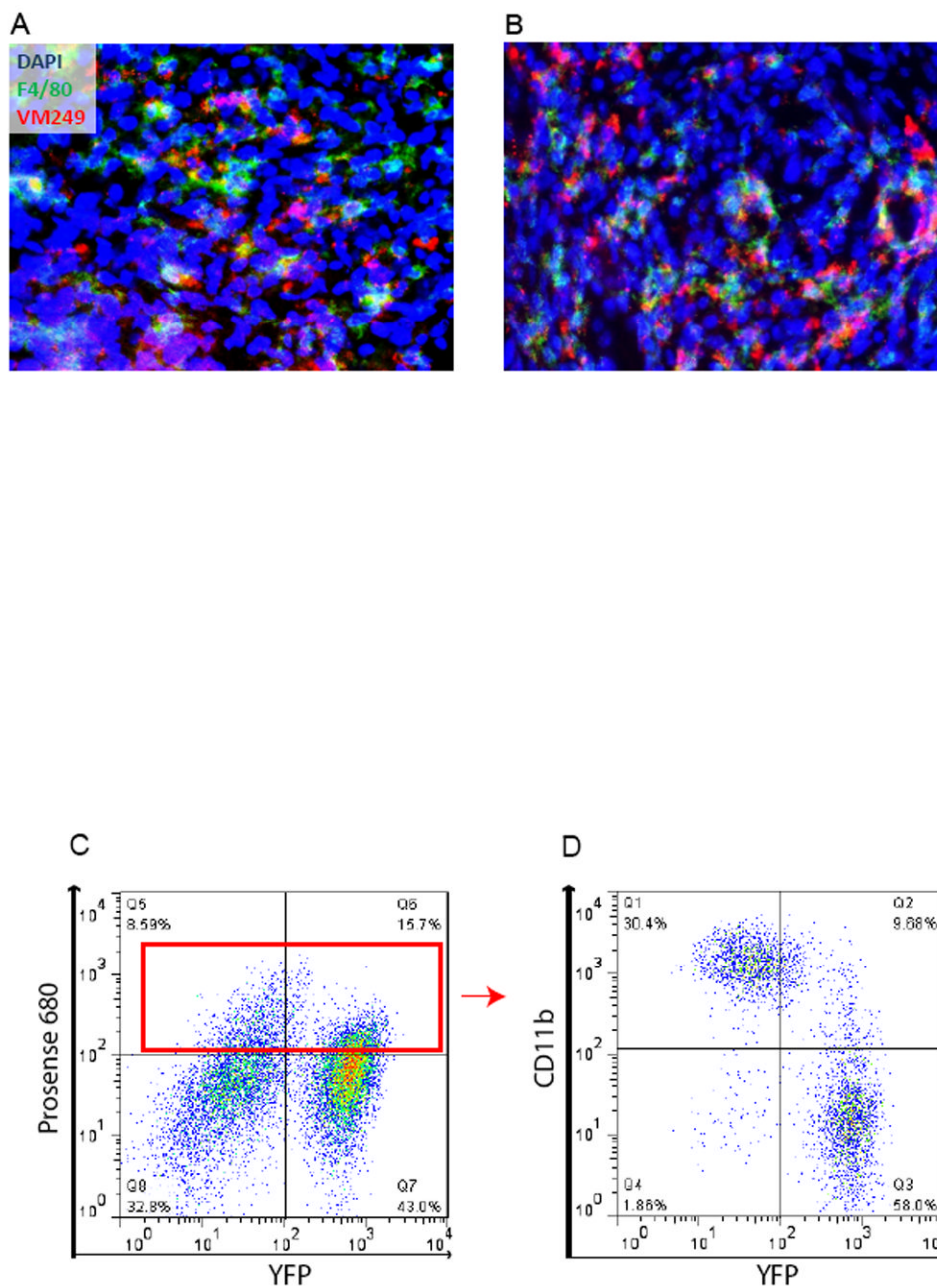


Figure 5. Probe activation and the tumor microenvironment. (A) Untreated mice or (B) mice treated with 5 Gy were injected with VM249 7 days after completion of RT. Tumors were harvested six hours after probe injection and unfixed tumor frozen sections were stained with the macrophage marker F4/80 and nuclear stain DAPI. (C) Sarcoma bearing *Rosa26^{YFP/YFP}*; *LSL-Kras^{G12D}*; *p53^{F/F1}* mice were injected with Prosense 680 and the tumor was removed 24 hours later. Cells from the tumor were stained for CD11b and sorted by flow cytometry (D).

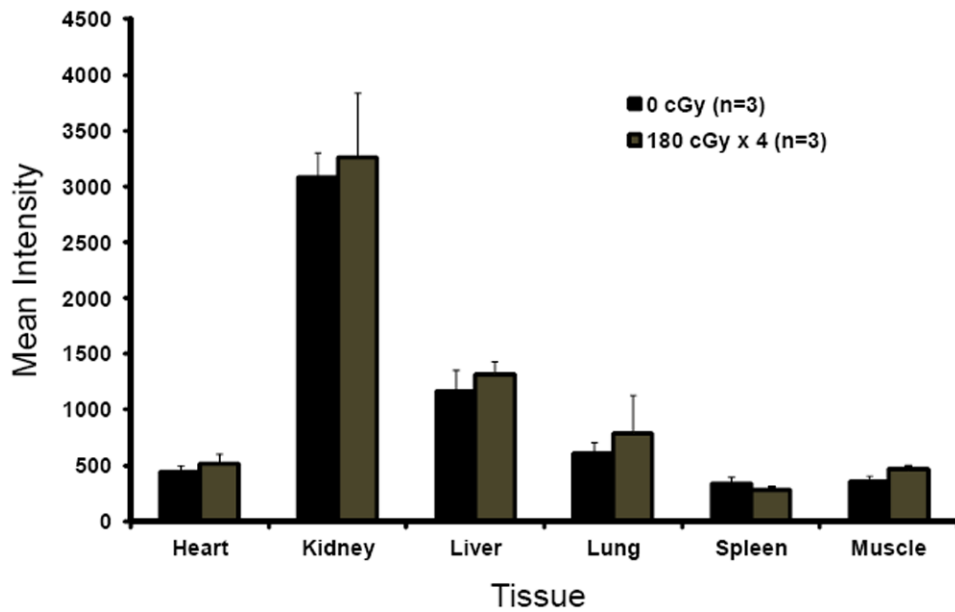


Figure 6. Background probe activation in different tissues is not affected by total body irradiation. Mice without tumors were treated with TBI to 0 Gy or 7.2 Gy in 180 cGy daily fractions and injected with VM249 one week later. The mice were sacrificed six hours after injection when individual organs were removed, washed in PBS, and imaged using the hand held device.